Control of electron localization in the dissociation of H_2^+ using orthogonally polarized two-color sequential laser pulses

Feng He*

Key Laboratory for Laser Plasmas (Ministry of Education) and Department of Physics, Shanghai Jiaotong University, Shanghai 200240, People's Republic of China

(Received 4 July 2012; published 20 December 2012)

Orthogonally polarized two-color sequential laser pulses are used to control the electron localization in the dissociation of H_2^+. The first single attosecond pulse, whose polarization axis is perpendicular to the molecular axis, excites H_2^+ from $1s\sigma_g$ to $2p\pi_u$, and the time-delayed infrared pulse, whose polarization axis is parallel to the molecular axis, steers the electron between two nuclei. The simulation of the time-dependent Schrödinger equation predicts the control degree of the electron localization can be up to 90% with the current laser technology. In this article, we reveal that the mechanism for this asymmetric localization is due to the mixture of $2p\pi_g$ and $2p\pi_u$, instead of $1s\sigma_g$ and $2p\sigma_u$ in the previous studies.

DOI: 10.1103/PhysRevA.86.063415 PACS number(s): 32.80.Rm, 42.65.Ky, 32.30.Jc, 34.80.Qb

The control of the electron localization in the dissociating molecule attracted great of interest in past years, mainly because such control may provide a way to selectively break and form molecular bonds in chemical reactions [1]. Several control strategies are raised [2] with the advent of new laser technologies [3]. The shorter laser pulses make the control strategy work in the femtosecond time scale, and even in the attosecond time scale, most recently. In 2004, Roudnev *et al.* [4] proposed the use of a few-cycle phase-stabilized femtosecond laser pulse to steer the electron between nuclei during the dissociation of H_2^+ and HD^+, which has been realized in experiment by Kling *et al.* [5]. To track the dynamics of the asymmetric localization, the attosecond pulse is much needed since the time scale for the electron hopping between nuclei is subfemtoseconds. Bandrauk *et al.* [6] suggested that the electron hopping between two nuclei induced by the infrared laser pulse can be detected by the attosecond laser pulse. In 2007, He *et al.* [7] used the single attosecond pulse plus the time-delayed few-cycle phase-stabilized femtosecond pulse to control the excitation and the electron localization, and they predicted the electron localization can be controlled in an unprecedented high degree by changing the time delay between two pulses. This prediction has been achieved in experiment by Sansone *et al.* [8] in 2010. Most recently, Znakovskaya *et al.* [9] developed the control technique to the few-cycle midinfrared laser pulse. Though studies about the electron localization have been extended to bigger molecules, such as carbon monoxide [10,11], H_2^+ is still the favorite target of theoreticians for its simplicity.

Generally, the electron localization depends on the laser parameters [12,13], nuclear masses [7], and kinetic energy release of fragments [14–16]. We may have two illustrations to understand the asymmetric electron localization in the dissociation of H_2^+. The first one is based on the quantum interference of $1s\sigma_g$ and $2p\sigma_u$ states [13,17–19]. In this illustration, the relative phase between these two states decides which nucleus has the larger probabilities to capture the electron, and the relative probability of the two states decides the asymmetric degree. The second illustration is semiclassical [7,20,21]. It says that the electron localization is frozen when the growing interatomic barrier is high enough to stop the electron hopping between two nuclei in the attosecond time scale.

However, the physical explanation of the electron localization inside H_2^+ is still far from being completely discovered. Is the asymmetric electron localization in the dissociation of H_2^+ always due to the superposition of $1s\sigma_g$ and $2p\sigma_u$? Is it possible to selectively excite the molecule to the π orbits and to control the electron localization in the following dissociation? Are there some general control methods which can be extended to bigger molecules directly? In this article, we raise a new strategy to control the electron localization using orthogonally polarized two-color pulses. The polarization axis of the first ultraviolet (UV) pulse is perpendicular to the molecular axis. The time-delayed infrared (IR) laser pulse, whose polarization axis is parallel to the molecular axis, steers the electron between two nuclei during the dissociation. Different from before, where only the two lowest molecular orbits are involved [5,17,18,22], more states participate in this dynamics. This strategy can be practiced with the current laser technology, and can be applied to many big molecules.

We solve the time-dependent Schrödinger equation in the Cartesian coordinate (atomic units, $e = m = \hbar = 1$ are used unless indicated otherwise):

$$i\frac{\partial}{\partial t}\Psi(x,z,R;t) = (H_0 + H_I)\Psi(x,z,R;t), \tag{1}$$

where H_0 is the field-free Hamiltonian:

$$H_0 = -\frac{1}{2M}\frac{\partial^2}{\partial R^2} - \frac{1}{2}\frac{\partial^2}{\partial x^2} - \frac{1}{2}\frac{\partial^2}{\partial z^2} + \frac{1}{R} - \sum_{\pm}\frac{1}{\sqrt{x^2 + (z \pm R/2)^2 + s}}, \tag{2}$$

and H_I is the coupling between the electron and external fields:

$$H_I = xE_{\mathrm{UV}}(t) + zE_{\mathrm{IR}}(t), \tag{3}$$

where M is the reduced nuclear mass and $M = 918$. We introduce the soft-core parameter s to remedy the Coulomb singularity. By setting $s = 0.64$, we obtain the ground-state energy -0.59 and the equilibrium internuclear distance 3. Note

*fhe@sjtu.edu.cn

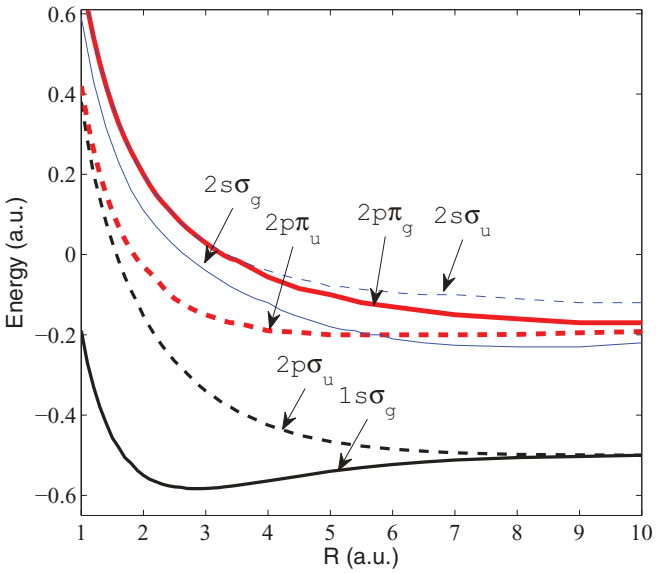

FIG. 1. (Color online) The potential curves of several quantum states within the Born-Oppenheimer approximation.

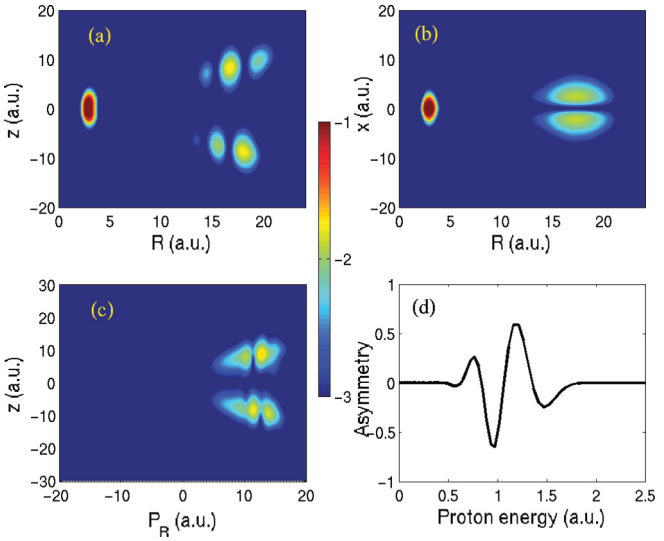

FIG. 2. (Color online) The logarithmic distribution of the wave function in the representations (a) (R,z), (b) (R,x), and (c) (P_R,z). (d) The asymmetry parameter as a function of the proton energy. The time delay is $\Delta t = 500$ and the CEP is $\theta = 0$. The snapshots are taken at $t = 1350$.

that the R-dependent soft-core parameter [23] would be helpful to obtain a more realistic equilibrium internuclear distance. We neglect the rotation of the molecule. Since the dynamics of the electron, including the coupling with two nuclei and the external fields, all happen in the x-z plane, it is a reliable approximation to ignore the expansion of the wave packet in the y dimension. In the simulation, the spatial grids are $\delta x = \delta z = 0.3$ and $\delta R = 0.04$, and the time step is $\delta t = 0.15$. The grids in the x, z, and R dimensions are 300, 300, and 1000, respectively. To suppress the unphysical reflection from the simulation borders, we introduce the mask function [7] in the border of the simulation box. Actually, this mask function is only used to absorb the ionized fragments, as the simulation box is big enough that the dissociative wave packets have not yet reached the borders by the end of our calculations. We tested and found that no observable reflections come from the borders in all the simulations. Both the UV and IR laser fields in our simulations are expressed, respectively, as follows:

$$E_{\rm UV} = E_{0,\rm UV}\sin(\omega_{\rm UV}t)\sin^2\left(\frac{\pi t}{\tau_{UV}}\right), \quad t \in [0,\tau_{\rm UV}], \tag{4}$$

$$E_{\rm IR} = E_{0,\rm IR}\sin[\omega_{\rm IR}(t-\Delta t)+\theta]\sin^2\left[\frac{\pi(t-\Delta t)}{\tau_{\rm IR}}\right], \quad t \in [\Delta t, \Delta t+\tau_{\rm IR}]. \tag{5}$$

The intensity and wavelength for the UV (IR) pulse are 10^{14} W/cm^2 (10^{12} W/cm^2) and 100 nm (800 nm), respectively. θ is the carrier envelope phase (CEP) of the IR pulse. Both UV and IR pulses contain four cycles, i.e., $\tau_{\rm IR} = 8\pi/\omega_{\rm IR}$ and $\tau_{\rm UV} = 8\pi/\omega_{\rm UV}$.

Taking R as a static parameter in Eq. (1), we calculate the potential surfaces of several quantum states. Figure 1 presents the molecular energy as a function of the internuclear distance for several states. Several excited states, such as $2p\sigma_u$, $2p\pi_u$, $2p\pi_g$, $2s\sigma_g$, and $2s\sigma_u$, are marked in the figure. The molecular excitation depends sensitively on the laser parameters, among which the cross angle between the molecular axis and the laser polarization axis plays a very important role [24–26]. When the polarization axis of the UV pulse is perpendicular to the molecular axis, the molecule is very likely to be excited from the $1s\sigma_g$ to the $2p\pi_u$ state if the photon energy is proper. However, if the laser polarization axis parallels the molecular axis, the transition between $1s\sigma_g$ and $2p\sigma_u$is dominant.

In our strategy, we first use the UV pulse to excite the molecule from the $1s\sigma_g$to the $2p\pi_u$ state, resulting in the dissociation. Then, a time-delayed IR field will steer the electron between two nuclei. After the IR field is off, we propagate the wave function continuously until the nuclear momentum and the electron localization are converged. The wave-function distribution $W(z,R;t)$ and $W(x,R;t)$ in the (z,R) and (x,R) spaces are, respectively,

$$W(z,R;t) = \int dx|\Psi(x,z,R;t)|^2, \tag{6}$$

$$W(x,R;t) = \int dz|\Psi(x,z,R;t)|^2. \tag{7}$$

Figures 2(a) and 2(b) show $W(z,R;t)$ and $W(x,R;t)$, respectively, when $t = 1350$. The time delay is $\Delta t = 500$. The bound states, locating in the regions $R < 8$, are clearly separate from the dissociative states. The node in the vicinities of $x = 0$ in (x,R) space confirms that the electron is in the π orbit. The dissociative states in the (z,R) space present distinct interference patterns along the R axis. Following the movie [27], we may clearly see that at first the UV pulse launches the dissociating wave packet without the interference structure; however, the time-delayed IR field repeatedly drives the electron back and forth between two nuclei, bringing in the interference structures. One may clearly see that the electron localization on both nuclei depends on the internuclear distance sensitively, where the internuclear distance reflects the nuclear momentum.

To directly look into the dependence of the electron localization on the nuclear momentum P_R, we first project out

the vibrational states and then only transform the dissociative states into the phase space (x,z,P_R). The obtained wave function is written as $\tilde{\Psi}(x,z,P_R;t)$, and its distribution in (z,P_R) space is

$$W(z,P_R;t) = \int dx|\tilde{\Psi}(x,z,P_R;t)|^2. \quad (8)$$

Figure 2(c) shows $W(z,P_R;t)$ at $t = 1350$. At this moment, P_R is already converged. Accordingly, the dependence of the electron distribution on the proton energy may be written as

$$W(z,E_R;t) = \int dx|\tilde{\Psi}(x,z,P_R;t)|^2/|P_R|, \quad (9)$$

where $E_R = P_R^2/4M$ is the individual proton energy.

To express the degree of the asymmetry, we define the asymmetry parameter as

$$A(E_R) = \frac{Q_1(E_R) - Q_2(E_R)}{Q_1(E_R) + Q_2(E_R)}, \quad (10)$$

where

$$Q_1(E_R) = \int_0^{+\infty} dz\, W(z,E_R;t), \quad (11)$$

$$Q_2(E_R) = \int_{-\infty}^{0} dz\, W(z,E_R;t). \quad (12)$$

Here t must be large enough to guarantee the convergency of all the detectable quantities. Figure 2(d) shows the asymmetry parameter as a function of proton energies, where all the parameters are the same as those in Fig. 2(c). The very large amplitude shows the strong dependence of the electron localization on the proton energy.

The asymmetry parameter may be controlled by the laser parameters, such as the CEP θ and the time delay Δt between UV and IR pulses. Figure 3(a) shows the dependence of the asymmetry parameter as functions of the proton energy E_R and θ when the time delay is fixed at $\Delta t = 500$. Similarly, by fixing $\theta = 0$ while tuning the time delay Δt, we may obtain the dependence of the asymmetry parameter as functions of the proton energy and the time delay, as shown in Fig. 3(b). The simulation results show the control degree is up to 90% for the proper laser parameters. The asymmetry varies periodically with Δt, θ, and E_R, as shown by the stripes in Figs. 3(a) and 3(b).

Similar to the superposition of $1s\sigma_g$ and $2p\sigma_u$ resulting in the asymmetric localization, the mixture of $2p\pi_g$and $2p\pi_u$ is responsible for the asymmetric localization in this control strategy. Figures 4(a) and 4(b) show the $2p\pi_g$ and $2p\pi_u$ wave function when the internuclear distance is set at $R = 10$. The superposition states $2p\pi_g - 2p\pi_u$and $2p\pi_g + 2p\pi_u$ are shown in Figs. 4(c) and 4(d), respectively. Comparing with Figs. 2(a) and 2(b), or following the wave function evolution [27], we may conclude that the IR field exchanges $2p\pi_g$ and $2p\pi_u$states and builds a superposition $\alpha(t)2p\pi_g + \beta(t)2p\pi_u$, resulting in asymmetric localization. Here the complex time-dependent amplitudes $\alpha(t)$ and $\beta(t)$ govern the relative phase and relative probability between the two states. In the IR field-dressed H_2^+, the electron is hopping between two nuclei with the Rabi frequency. When the laser field is off and the internuclear distance is very large, the energies of $2p\pi_g$ and $2p\pi_u$ states almost degenerate, so the electron hopping ceases. Comparing with the dissociation directly from $2p\sigma_u$, the fragment dissociating through $2p\pi_u$ gains smaller kinetic energies. Moreover, the energy gap between $2p\pi_g$ and $2p\pi_u$ varies slowly with the internuclear distance. According to the above two factors, the IR field may steer the electron very effectively within several optical cycles, making the interference pattern in Fig. 2(a) very distinct.

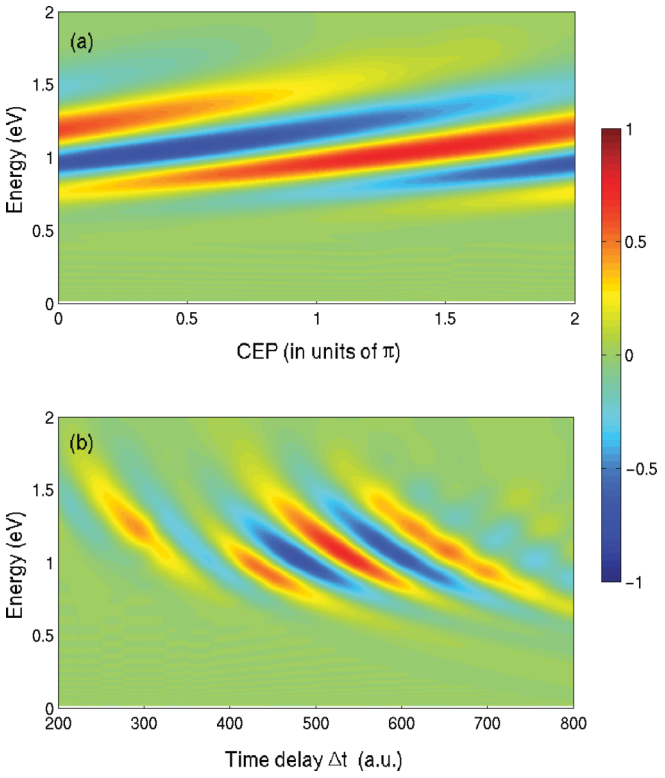

FIG. 3. (Color online) (a) The asymmetry parameter as functions of the CEP and proton energy when the time delay is fixed at $\Delta t = 500$. (b) The asymmetry parameter as functions of the time delay and proton energy when the CEP is fixed at $\theta = 0$.

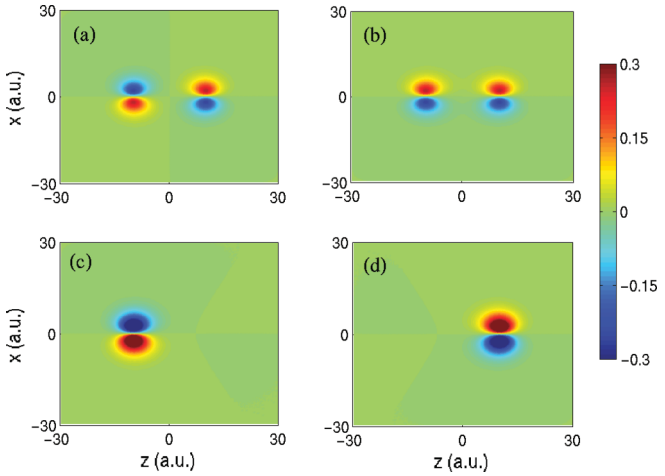

FIG. 4. (Color online) Molecular orbits. (a) $2p\pi_g$, (b) $2p\pi_u$, (c) $2p\pi_g - 2p\pi_u$, and (d) $2p\pi_g + 2p\pi_u$.

After accepting the principle of the superposition of $2p\pi_g$ and $2p\pi_u$, we may refer back to the slopes of the stripes in Figs. 3(a) and 3(b). Fundamentally, the asymmetry parameter is governed by the phase term $\omega_{\rm IR}(t-\Delta t)+\theta$. For the components of the dissociating nuclear wave packets with different momenta, they reach $R_{\rm resonant}$ at different moments, where $R_{\rm resonant}$ is the internuclear distance at which the energy gap between $2p\pi_u$ and $2p\pi_g$ is equal to the IR photon energy, therefore the resonant transition between the two states happens. The component with the higher kinetic energy arrives at $R_{\rm resonant}$ earlier, which is equivalent to being dressed by an IR field with a smaller time delay Δt or, alternatively, with a larger CEP θ. Consequently, the associations of the higher kinetic energy and the larger CEP, or the higher kinetic energy and the larger time delay, are expressed by the positive and negative slopes of the stripes in Figs. 3(a) and 3(b), respectively.

By directly counting on the probability on two nuclear sides, one may obtain the energy-independent asymmetry parameter

$$B=\frac{\int[Q_1(E_R)-Q_2(E_R)]dE_R}{\int[Q_1(E_R)+Q_2(E_R)]dE_R}. \tag{13}$$

Our simulations with the same parameters in Fig. 3 show that B is always very close to 0 for all the time delays and CEPs. This phenomenon can be explained intuitively by the aid of the interatomic barrier in the classical picture. Note that the evolution of $\alpha(t)2p\pi_g+\beta(t)2p\pi_u$ represents the classical hopping between two nuclei. If the IR pulse is exerted when the internuclear distance is small and the interatomic barrier is low, the electron is driven by the IR field back and forth, in which process the low interatomic barrier does not affect the electron motion obviously. The actions of the first and second half IR optical cycles nearly cancel out, resulting in the symmetric electron localization. If the laser pulse is introduced very late, when the internuclear distance of the dissociating nuclear wave packets is very large and the interatomic barrier is high enough to block the electron movement, the electron localization is similar to the case that no IR field is added. If the IR field is introduced by the time the dissociating nuclear wave packet reaches $R=17$, where the interatomic barrier crosses the $2p\pi_u$ potential curve, the quiver radius of the electron in such a laser field (10^{12} W/cm^2, 800 nm) is much smaller than 17, so that the laser field hardly drives the electron from one nucleus to the other and the symmetric localization is preserved. However, in Refs. [7,14,20] the interatomic barrier crosses the $2p\sigma_u$ potential curve at $R=6.3$, in which case the interatomic barrier works as an ultrafast shutter to block the electron motion and freeze the electron localization finally.

In the current strategy, to amplify the quiver radius to allow the electron hop between two nuclei with $R\sim 17$, we may increase the laser intensity or use the pulse with the longer wavelength. In order to avoid the ionization, we fix the laser intensity at 10^{12} W/cm^2 but lengthen the wavelengths to 2400 and 3200 nm, and our simulations show the energy-independent asymmetry parameter B can be up to 0.08 and 0.1, respectively. This analysis is consistent with the quantum mechanical explanation, in which frame the pulse with a longer wavelength or higher intensity is also necessary to make a substantial transition between $2p\pi_g$ and $2p\pi_u$ at $R\sim 17$ since the energy gap is already very small.

It is worth emphasizing that our control strategy is clearly different from all the existing methods. In the old methods, only the two lowest states, i.e., $1s\sigma_g$ and $2p\sigma_u$, are involved in the dissociative process, therefore the two-state model almost presents the same simulation results with the full quantum simulations if the ionization may be neglected. However, in our strategy, the attosecond pulse directly excites H_2^+ from $1s\sigma_g$ to $2p\pi_u$, and completely skips $2p\sigma_u$. Totally, three states are involved in the process although the later dynamics is not relevant to $1s\sigma_g$ anymore. The current laser technology is ready to examine our predictions.

In conclusion, the orthogonally polarized two-color laser pulses can be used to effectively control the electron localization during the dissociation of H_2^+. The electron localization depends on the time delay between UV and IR pulses, the CEP of the IR pulse, and the proton energy. In the quantal picture, the IR pulse builds the superposition of $2p\pi_u$ and $2p\pi_g$, and such two-state interference causes the preference (as high as 90%) of the electron localization. In the complementary classical picture, the interatomic barrier does not break the symmetry appreciably, therefore, the total probabilities on each nucleus are almost equal. Though the CEP and time delays between pulses have been studied extensively, we bring in the third parameter, the polarization direction, as the robust controlling protocol for the electron localization. This strategy is even greater for the control of the electron localization during the dissociation of bigger molecules, such as O_2^+ [28,29] and N_2^+ [30,31], in which the π orbit plays an important or even decisive role.

This work was supported by the Pujiang scholar funding (Grant No. 11PJ1404800), NSF of Shanghai (Grant No. 11ZR1417100) and NSF of China (Grants No. 11104180 and No. 11175120), and the Fok Ying-Tong Education Foundation for Young Teachers in the Higher Education Institutions of China (Grant No. 131010).

[1] A. H. Zewail, J. Phys. Chem. A **104**, 5660 (2000).
[2] D. J. Tannor, *Introduction to Quantum mechanics: A Time-Dependent Perspective* (University Science Books, California, 2007).
[3] T. Babrec and F. Krausz, Rev. Mod. Phys. **72**, 545 (2000).
[4] V. Roudnev, B. D. Esry, and I. Ben-Itzhak, Phys. Rev. Lett. **93**, 163601 (2004).
[5] M. F. Kling *et al.*, Science **312**, 246 (2006).
[6] A. Bandrauk, S. Chelkowski, and H. Nguyen, Int. J. Quantum Chem. **100**, 834 (2004).
[7] F. He, C. Ruiz, and A. Becker, Phys. Rev. Lett. **99**, 083002 (2007).
[8] G. Sansone *et al.*, Nature (London) **465**, 763 (2010).
[9] I. Znakovskaya *et al.*, Phys. Rev. Lett. **108**, 063002 (2012).
[10] I. Znakovskaya, P. von den Hoff, S. Zherebtsov, A. Wirth, O. Herrwerth, M. J. J. Vrakking, R. de Vivie-Riedle, and M. F. Kling, Phys. Rev. Lett. **103**, 103002 (2009).

[11] Y. Liu, X. Liu, Y. Deng, C. Wu, H. Jiang, and Q. Gong, Phys. Rev. Lett. **106**, 073004 (2011).
[12] K. Liu, W. Hong, Q. Zhang, and P. Lu, Opt. Express **19**, 26359 (2011).
[13] F. Kelkensberg *et al.*, Phys. Rev. Lett. **107**, 043002 (2011).
[14] D. Ray *et al.*, Phys. Rev. Lett. **103**, 223201 (2009).
[15] M. Kremer *et al.*, Phys. Rev. Lett. **103**, 213003 (2009).
[16] B. Fischer, M. Kremer, T. Pfeifer, B. Feuerstein, V. Sharma, U. Thumm, C. D. Schroter, R. Moshammer, and J. Ullrich, Phys. Rev. Lett. **105**, 223001 (2010).
[17] E. Charron, A. Giusti-Suzor, and F. H. Meis, J. Chem. Phys. **103**, 7359 (1995).
[18] C. R. Calvert *et al.*, J. Phys. B **43**, 011001 (2010).
[19] S. Chatterjee, B. Dutta, and S. S. Bhattacharyya, Phys. Rev. A **83**, 063413 (2011).
[20] F. He, A. Becker, and U. Thumm, Phys. Rev. Lett. **101**, 213002 (2008).
[21] N. Takemoto and A. Becker, Phys. Rev. Lett. **105**, 203004 (2010).
[22] K. Singh *et al.*, Phys. Rev. Lett. **104**, 023001 (2010).
[23] B. Feuerstein and U. Thumm, Phys. Rev. A **67**, 043405 (2003).
[24] F. Kelkensberg, G. Sansone, M. Ivanov, and M. Varkking, Phys. Chem. Chem. Phys. **13**, 8647 (2011).
[25] X. M. Tong, Z. X. Zhao, and C. D. Lin, Phys. Rev. Lett. **91**, 233203 (2003).
[26] J. Hu, K. L. Han, and G. Z. He, Phys. Rev. Lett. **95**, 123001 (2005).
[27] See Supplemental Material at http://link.aps.org/supplemental/10.1103/PhysRevA.86.063415 for the two-color pulse and the time evolution of $W(z,R)$ and $W(x,R)$.
[28] M. Zohrabi *et al.*, Phys. Rev. A **83**, 053405 (2011).
[29] M. Magrakvelidze, C. M. Aikens, and U. Thumm, Phys. Rev. A **86**, 023402 (2012).
[30] B. Gaire, J. McKenna, A. M. Sayler, N. G. Johnson, E. Parke, K. D. Carnes, B. D. Esry, and I. Ben-Itzhak, Phys. Rev. A **78**, 033430 (2008).
[31] C. Figueira de Morisson Faria and B. B. Augstein, Phys. Rev. A **81**, 043409 (2010).